Visual Neuroscience (1996), **13**, 907-922. Printed in the USA.

Contributions of individual layer 2–5 spiny neurons to local circuits in macaque primary visual cortex

EDWARD M. CALLAWAY AND ANNE K. WISER
Molecular Neurobiology Laboratory, The Salk Institute for Biological Studies, La Jolla

(RECEIVED January 9, 1996; ACCEPTED March 11, 1996)

Abstract

We studied excitatory local circuits in the macaque primary visual cortex (V1) to investigate their relationships to the magnocellular (M) and parvocellular (P) streams. Sixty-two intracellularly labeled spiny neurons in layers 2–5 were analyzed. We made detailed observations of the laminar and columnar specificity of axonal arbors and noted correlations with dendritic arbors. We find evidence for considerable mixing of M and P streams by the local circuitry in V1. Such mixing is provided by neurons in the primary geniculate recipient layer 4C, as well as by neurons in both the supragranular and infragranular layers. We were also interested in possible differences in the axonal projections of neurons with different dendritic morphologies. We found that layer 4B spiny stellate and pyramidal neurons have similar axonal arbors. However, we identified two types of layer 5 pyramidal neuron. The majority have a conventional pyramidal dendritic morphology, a dense axonal arbor in layers 2–4B, and do not project to the white matter. Layer 5 projection neurons have an unusual "backbranching" dendritic morphology (apical dendritic branches arc downward rather than upward) and weak or no axonal arborization in layers 2–4B, but have long horizontal axonal projections in layer 5B. We find no strong projection from layer 5 pyramidal neurons to layer 6. In macaque V1 there appears to be no single source of strong local input to layer 6; only a minority of cells in layers 2–5 have axonal branches in layer 6 and these are sparse. Our results suggest that local circuits in V1 mediate interactions between M and P input that are complex and not easily incorporated into a simple framework.

Keywords: Macaque, V1, Striate cortex, Local circuits, Functional streams

Introduction

An important step toward understanding the neural mechanisms that give rise to visual perception is to obtain detailed descriptions of the circuits that underlie visual computations. Here we describe experiments aimed at obtaining a more detailed anatomical description of local circuitry in the primary visual cortex (V1) of macaque monkeys. We were particularly interested in interactions between the magnocellular (M) and parvocellular (P) streams that might be mediated by local circuitry in V1. Although there is little or no mixing of input from the M and P streams at earlier processing stages, there is considerable opportunity for convergence of input within V1 (see Merigan & Maunsell, 1993 for review).

Understanding the relationships between the independent M and P pathways that provide input to V1 and the distinct populations of neurons providing output to higher cortical areas requires information about local circuits arising from layer 4C and their relationships to layer 4B and to the cytochrome oxidase (CO) blobs and interblobs of layer 2/3. Past reports are in general agreement about the specificity of lateral projections within layer 2/3 from blobs to blobs or interblobs to interblobs (Livingstone & Hubel, 1984; McGuire et al., 1991; Lund et al., 1993). However, findings from studies addressing the relationship of projections from layer 4 to CO blobs in layer 2/3 are less consistent. Based on retrograde labeling following biocytin injections in blobs or interblobs of layer 3B, Lachica et al. (1992) report that blobs receive direct input from both the M and P geniculate recipient layers, 4Cα and 4Cβ, respectively, while interblobs receive input only from layer 4Cβ. On the other hand, Yoshioka et al. (1994) report that only interblobs receive direct input from layer 4C, and that this is provided by neurons in mid-4C. Also, although both groups agree that layer 4B neurons project primarily to blobs in layer 2/3, they disagree about the projections from the parvocellular recipient layer 4A; Lachica et al. (1992) report projections to both blobs and interblobs, while Yoshioka et al. (1994) report projections just to blobs. We were interested in determining whether these discrepancies might be related to technical differences that could be resolved by the use of a different method that is in some respects more sensitive (intracellular labeling), or instead might reflect genuine biological variability. Interactions between the M and P pathways could also be mediated by neurons in the infragranular layers, but there is little information about whether pro-

Reprint requests to: Edward M. Callaway, MNL-C, The Salk Institute for Biological Studies, 10010 N. Torrey Pines Rd., La Jolla, CA 92037, USA.

jections from these layers are specific for blob or interblob compartments in layer 2/3, or whether the positions of neurons that project to layer 4B have a particular relationship to overlying blobs.

Our analyses also allowed us to address other issues about the specificity of local circuits that were not clearly resolved by other methods. Although considerable detail about the organization of V1 local circuitry has been revealed previously (Lund, 1973; Lund & Boothe, 1975; Lund et al., 1977; Blasdel et al., 1985; Fitzpatrick et al., 1985; Valverde, 1985; Katz et al., 1989; Lachica et al., 1992; Anderson et al., 1993; Yoshioka et al., 1994), our understanding has been technically limited. Golgi staining gives a limited view of axonal arbors, and results from extracellular tracer injections are not straightforward to interpret. Also, such studies provide little information about the extent, diversity, or specificity of axonal arbors from individual neurons, or about correlations between dendritic and axonal arborization. Intracellular neuronal labeling can provide excellent dendritic and axonal labeling with single-cell resolution (Gilbert & Wiesel, 1979, 1983; Gilbert, 1983; Martin & Whitteridge, 1984; Martin, 1984), but the number of intracellularly labeled neurons from macaque V1 is still small (Katz et al., 1989; McGuire et al., 1991; Anderson et al., 1993; Usrey & Fitzpatrick, 1994). Using intracellular labeling, we were able to identify correlations between patterns of dendritic and axonal arborization that presumably reflect involvement of different neuronal types from the same layer in different neural circuits.

We used biocytin-filled patch electrodes to intracellularly label neurons in living coronal brain slices prepared from macaque striate cortex. The tissue was double stained for CO and biocytin to allow visualization of blobs and laminar boundaries in the same sections as labeled neuronal processes. Here we describe 62 pyramidal and spiny stellate neurons with somata in layers 2–5, which are presumed to contribute excitatory synapses (Saint Marie & Peters, 1985; McGuire et al., 1991). A separate paper describes analyses of 58 layer 6 pyramidal neurons (Wiser & Callaway, 1996). We have not labeled any neurons with somata in layer 1.

Methods

Individual neurons in the primary visual cortex of macaque monkeys were intracellularly labeled in living brain slices and their axonal and dendritic arbors analyzed as described below. We intracellularly labeled layer 2–5 neurons from a total of nine macaque monkeys (*Macaca radiata*) of both sexes. The age of each animal and the number of layer 2–5 spiny cells sampled from it are as follows: <5 h, $n = 3$ (all are layer 4Cβ spiny stellates); 1 week, $n = 1$ (a layer 4B pyramid); 3 months, $n = 6$; 3.5 months, $n = 7$; 5 months, $n = 7$; 6 months, $n = 28$; 8 months, $n = 5$; 9 months, $n = 4$; and 20 months, $n = 1$. We used young animals because it is much easier to obtain whole-cell recordings than in slices from older animals. Neurons of each type were similar in both axonal and dendritic morphology, regardless of the age of the animals from which they were sampled. However, layer 4Cβ neurons were sampled only in the youngest animal (see Results and Discussion). Slices from many of the animals, particularly those for which the number of labeled neurons was small, were also used for other investigations not described here.

Preparation of cortical slices

We prepared 400-μm thick coronal slices from the striate cortex using methods essentially identical to those described previously for cats (Katz, 1987; Callaway & Katz, 1992) and monkeys (Katz et al., 1989). Briefly, animals were deeply anesthetized with sodium pentobarbital (40–60 mg/kg, i.p.) and a large craniotomy was made to expose the striate cortex. The dura was removed and a large portion of the striate cortex (approximately 2 cm wide and 2.5 cm long) was cut free with a scalpel and removed. This tissue was then placed in chilled (about 2°C), oxygenated artificial cerebrospinal fluid (ACSF, composition in mM: NaCl, 124; KCl, 5; KH_2PO_4, 1.25; $MgSO_4$, 2; $CaCl_2$, 3; $NaHCO_3$, 26; *d*-glucose, 10; kynurenic acid, 1; pH 7.4). The animal was overdosed with an additional dose of sodium pentobarbital (100 mg/kg, i.p.) following removal of the cortex. After chilling for about 1 min, the cortical tissue was placed on filter paper saturated with ACSF, the pia was removed with fine forceps, and the tissue was cut into two blocks, each about 6–8 mm wide and 2 cm long, that were then sliced coronally to a thickness of 400 μm using a specialized "egg slicer"-like device (Katz, 1987). This procedure yielded more than 100 slices of which 40–60 were typically stored in oxygenated interface chambers warmed to 34°C, for later intracellular filling. These slices originated from positions distributed over nearly the entire exposed surface of area V1—anteriorly from the V1/V2 border to the occipital pole posteriorly, and mediolaterally from the midline to about 2.5 cm laterally. Thus labeled neurons in our sample are not localized to any particular representation of the visual field, with the exception that regions corresponding to tissue folded beneath the exposed surface of the brain were not sampled.

Intracellular labeling

After incubating in the interface chamber for at least 1 h, slices were transferred to a recording chamber where they were submerged in warm (34°C), oxygenated ACSF circulating at a rate of about 2 ml/min. Whole-cell recordings were obtained in either voltage-clamp or current-clamp mode using methods similar to those described previously (Blanton et al., 1989). The electrodes used had resistances of 5–15 MΩ and were filled with the following solution: 130 mM potassium gluconate, 1 mM EGTA, 2 mM $MgCl_2$, 0.5 mM $CaCl_2$, 2.54 mM ATP, 10 mM HEPES, and 2% biocytin (Sigma Chemical Co., St. Louis, MO), pH 7.3. After a whole-cell recording was obtained, biocytin was iontophoresed into the cell with positive current pulses of 0.3 nA and 33-mS duration at 10Hz.

Cells were typically filled for at least 10 min and this procedure invariably resulted in complete filling of the axonal and dendritic arbors (see Fig. 1). Occasionally, recordings were lost after shorter periods, but the filling was often excellent despite the shorter filling duration. Only neurons in which the entire dendritic and axonal arbor could be clearly visualized and reconstructed following staining are included in our analyses. The cell bodies of some neurons are surrounded by a cloud of label (Figs. 1b and 1c). This presumably results from leakage of biocytin from the pipette during whole-cell recording and/or biocytin forced out of the pipette by positive pressure prior to the formation of a GΩ seal. Regardless of the cause, this does not interfere with our analyses. Fine details of dendritic and axo-

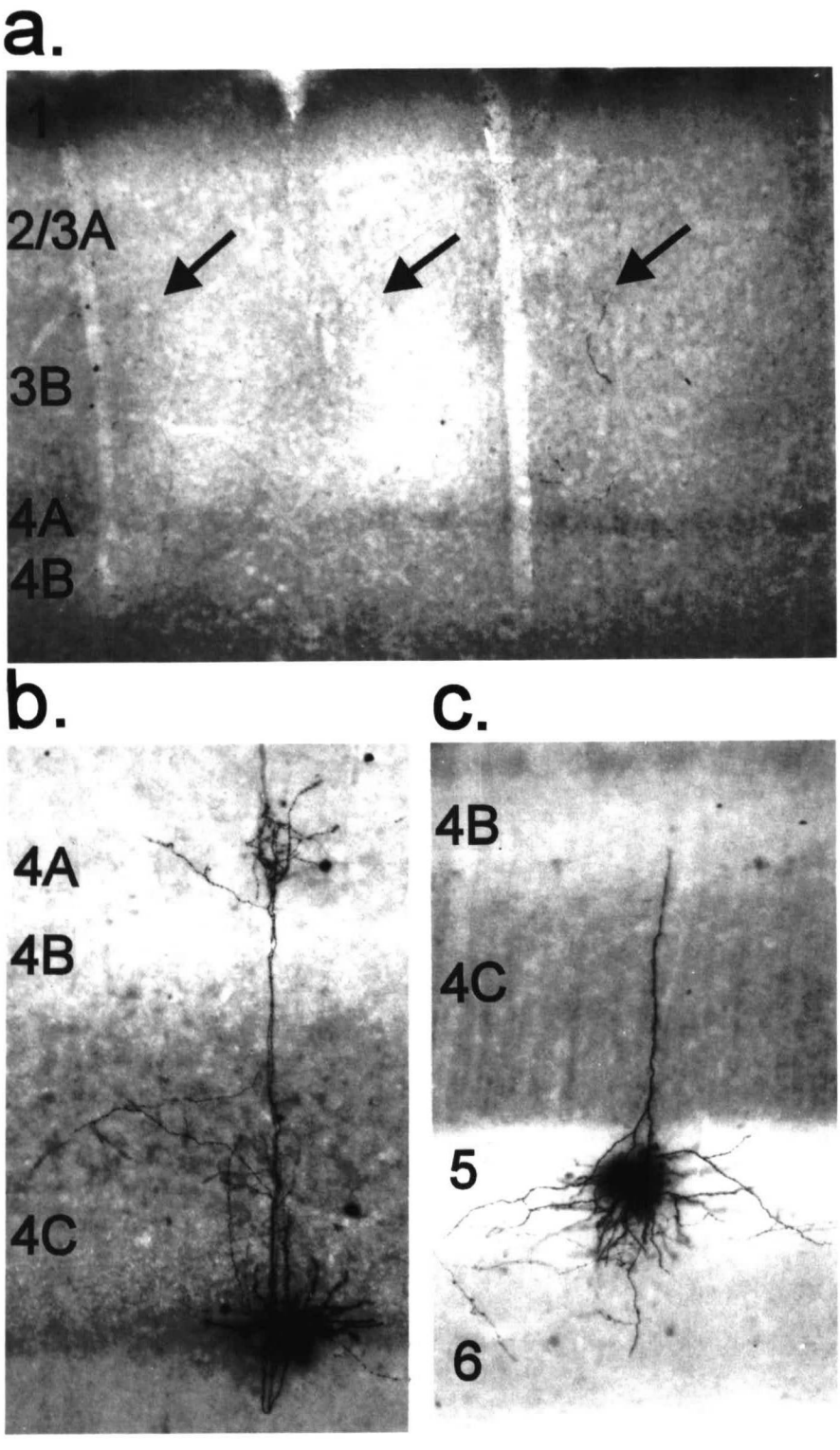

Fig. 1. Photographs of sections from V1 slices that have been double stained for CO and biocytin. Layers are identified by numbers at the left of each photograph. (a) Photograph illustrating dark-staining CO blobs (arrows) and lighter interblobs in layer 2/3. (b) Biocytin-labeled layer 4Cβ spiny stellate neuron with its cell body at the base of layer 4C. The dendrites are thicker than the axon and the basal dendrites curve upward, away from the 4C/5 border. The axon curves upward soon after leaving the base of the cell body and divides into branches that project to layers 4Cα, 4A, and 3B. The camera lucida reconstruction of this neuron is shown in Fig. 2a. (c) Biocytin-labeled layer 5 pyramidal neuron. The apical dendrite extends to the 4Cα/4B border. It has two "backbranching" collaterals that extend laterally and branch further in layer 5. The basal dendrites also extend relatively far laterally in layer 5. Axonal branches projecting down into layer 6 and extending laterally in layers 5 and 6 are also visible. The reconstruction of this neuron is shown in Fig. 13b.

nal processes can be visualized within the cloud by using a high-power objective and bright illumination with a stopped-down aperture. For example, compare the photographs of neurons in Figs. 1b and 1c with their reconstructions in Figs. 2a and 13b, respectively.

Electrode penetrations into the slice were spaced such that labeled neurons would be at least 1 mm apart laterally. After several neurons in a slice were labeled, it was returned to the interface holding chamber for about 2–6 h. This postincubation procedure resulted in removal of nonspecific labeling at the locations of electrode penetrations, that would otherwise obscure the processes of specifically labeled neurons. Following postincubation, slices were fixed by immersion in 4% paraformaldehyde in 0.1 M phosphate buffer for 12–14 h. The short fix-

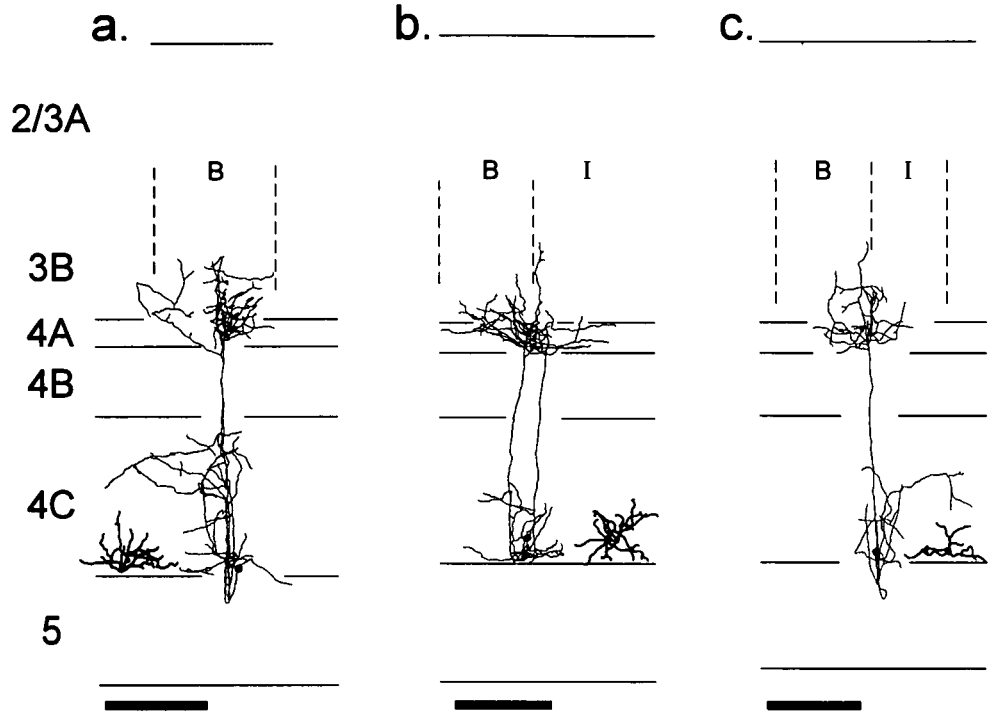

Fig. 2. Camera lucida reconstructions of layer 4Cβ spiny stellate neurons. Axonal arbors (fine lines) are illustrated in their actual positions and originate from the cell body as indicated by the filled figures. Dendrites (in bold) are shown at the same scale, but are offset to the side in order to avoid obscuring the axonal arbors. Horizontal lines indicate the laminar boundaries of the different cortical layers labeled on the left side. Vertical dotted lines indicate transitions between blob (B) and interblob (I) compartments in layer 2/3. All three spiny stellate cells project axonal branches to layers 4Cβ, 4A, and 3B. The neuron shown in (a) also projects to layer 4Cα. Its projection to layer 3B is predominantly within a blob and its soma is centered underneath this blob. The somata of the neurons in (b) and (c) are directly underneath blob/interblob transitions and the cells project axonal branches to both compartments in layer 3B. The dendrites of all three cells are restricted to layer 4Cβ. [Note the asymmetric dendritic arbors of the neurons in (a) and (c).] These neurons do not project to the white matter. A photograph of the neuron illustrated in (a) is shown in Fig. 1b. Scale bars (thick horizontal bars) = 200 μm.

ation time was crucial for obtaining good-quality CO staining (see below); shorter fixation times did not result in adequate tissue preservation.

Tissue processing

Following fixation, slices were sunk in 30% sucrose in 0.1 M phosphate buffer and then sectioned on a freezing microtome to a thickness of 50–100 μm. Sections were rinsed three times in phosphate-buffered saline (PBS) and then stained for CO by incubation in a solution containing 30 mg cytochrome-C, 20 mg catalase, and 50 mg diaminobenzidine (DAB, all from Sigma Chemical Co., St. Louis, MO) per 100 ml of PBS, for 2–4 h at 40–50°C (Horton, 1984). Sections were rinsed again, three times in PBS, and then incubated in 10% methanol and 3% H_2O_2 in PBS for 30 min. This step inactivates endogenous peroxidases commonly associated with blood vessels in the unperfused brain tissue. The sections were rinsed again, five times in PBS, and then incubated in a horseradish peroxidase (HRP)-conjugated avidin-biotin complex (ABC, Vector Labs, Burlingame, CA; Peroxidase Standard Kit) prepared at the standard concentration in PBS and 0.75% Triton X-100, for 2 h. Sections were rinsed three times in PBS, submerged in 0.1% glutaraldehyde in PBS for 4 min (to reduce background staining), and then rinsed five times in PBS. Finally, the intracellularly injected biocytin was revealed by reacting the sections in a solution containing 50 mg DAB, 2.8 ml of 1% cobalt chloride, 2.0 ml of 1% nickel ammonium sulfate, and 10 μl of 30% H_2O_2 per 100 ml of PBS for 5–15 min. This procedure resulted in a dense black reaction product in labeled neurons, against the reddish-brown reaction product from the CO stain (see Fig. 1).

Determination of laminar boundaries

Laminar boundaries were defined on the basis of the pattern of CO staining in each section, as indicated in Fig. 1. The criteria used were similar to those of Lund (1987, 1988). The most distinct laminar feature in the CO-stained tissue is layer 4C, which is the most densely stained region in the middle of the cortex. The subdivisions of this layer, 4Cα and 4Cβ, are not distinguished by the CO stain and we therefore define the upper half of layer 4C as 4Cα and the lower half as 4Cβ. Superficial to layer 4C is a lightly stained zone, layer 4B, and a thin darker staining band, layer 4A. Layer 1 is a thin CO dense zone just beneath the pial surface. We refer to the region between layer 4A and layer 1 as layer 2/3 and further subdivide this region into layers 2/3A (the upper two thirds) and 3B (the lower one third). Layer 5 is a lightly stained zone just below layer 4C and it is separated from the white matter by the darker-staining layer 6. Layer 5 is divided into an upper region, layer 5A (the upper

one third of layer 5), and a lower region, layer 5B (the lower two thirds of layer 5). The border between layer 6 and the white matter is marked by a sharp decrease in the intensity of CO staining. CO staining also distinguishes the blob and interblob regions in layer 2/3 (see Fig. 1a).

Analyses of intracellularly labeled neurons

Stained sections were scanned at 100× magnification (10×, 0.5 N.A. objective) to locate labeled neurons, and suitably labeled cells were identified. Such cells were labeled well enough that even the most distal axonal processes could easily be seen with the 10× objective (see Fig. 1). Each neuron was then carefully scrutinized at variable magnification to determine in detail its patterns of axonal and dendritic arborization and their relation to the cortical layers and CO blob and interblob regions of layer 2/3. Each neuron was also investigated to determine whether its main descending axon projected to the white matter. When the axon could be seen entering the white matter, the cell was scored as a projection neuron. Neurons were scored as nonprojecting only if the descending axon clearly ended within the plane of the slice. If the descending axon left the plane of the slice before entering the white matter, the cell was scored as ambiguous.

Our description below is based on observations of 62 well-labeled, layer 2–5 spiny neurons. For illustrative purposes, 28 representative neurons were reconstructed by camera lucida drawing. Detailed drawings of axonal arbors were made using a 60× or 63× (1.4 N.A.) oil immersion objective. Crude dendritic drawings were made using a 10× or 20× objective; the thickness of dendrites and other details such as dendritic spines are not indicated in these drawings, but all dendritic branches are shown. Camera lucida drawings were photographed with a large format camera and photographic prints made from the negatives. The prints were then scanned electronically using a PC-based computer system. Scale bars and hand-drawn lines indicating laminar and blob/interblob borders were replaced with computer drawn lines at their original positions on the scanned images, using the program CorelDraw.

Results

Overview

We have analyzed the patterns of axonal and dendritic arborization of 62 spiny neurons with cell bodies in layers 2–5 of macaque primary visual cortex. These neurons are classified according to the layer in which the cell body is located. The sample includes the following numbers of neurons from each layer: layer 4Cα, $n = 6$; layer 4Cβ, $n = 3$; layer 4B, $n = 15$; layer 4A, $n = 5$; layer 3B, $n = 8$; layer 2/3A, $n = 9$; and layer 5, $n = 16$. We will first describe neurons from the main geniculate recipient layer, 4C, then those from the more superficial layers that receive the strongest input from layer 4C, and finally those from layer 5 which receives its strongest input from the superficial layers.

Spiny stellate neurons of layer 4C

Of all the neurons in primary visual cortex, those in layer 4C proved to be the most difficult to fill intracellularly using whole-cell recording methods. Thus, the size of our sample from this layer is small relative to the numbers labeled in other layers. We obtained staining meeting our criteria (see Methods above) for a total of nine layer 4C spiny stellate neurons (see Figs. 1b and 2–4). Of these, the cell bodies of six are in layer 4Cα, and the remaining three are in 4Cβ. None of these cells projects its axon to the white matter.

Spiny stellates of layer 4Cβ

We sampled only three spiny stellate neurons in layer 4Cβ and all were from the youngest animal (<5 h old). Nevertheless, our observations of these neurons provide insight into the contributions of layer 4Cβ spiny stellates to V1 local circuitry. All three neurons have a spiny stellate dendritic morphology (Figs. 1b and 2), but two neurons with cell bodies near the bottom of layer 4Cβ have asymmetric dendritic arbors that do not penetrate into layer 5 (Figs. 1b, 2a and 2c). All three neurons in our sample have numerous axonal branches in layers 4Cβ, 4A, and 3B. None project to deeper layers. One neuron (Figs. 1b and 2a) also has a substantial axonal projection to layer 4Cα.

Beyond these observations, we were particularly interested in the relationships of the axonal arbors within layer 3B to CO blobs, and whether neurons at the bottom of layer 4Cβ project axons to layer 3B. These interests arise from the conflicting reports of Lachica et al. (1992), who report projections from layer 4Cβ to both blobs and interblobs, and Yoshioka et al. (1994) who report projections only to interblobs, and only from neurons in the upper half of layer 4Cβ.

The three layer 4Cβ neurons in our sample provide some insight into these issues. First, two of the neurons in our sample (Figs. 2a and 2c) have somata at the base of layer 4Cβ, and both have substantial axonal projections to layer 3B. In addition, all three neurons in our sample project to blobs in layer 3B. Two of the three cells also project to interblobs (Figs. 2b and 2c). We suspect that stronger projections to interblobs would be observed if neurons with somata directly under interblobs were labeled (see Discussion).

Spiny stellates of layer 4Cα

We have labeled and analyzed six spiny stellate neurons with somata in layer 4Cα (Figs. 3–4). These were all sampled from animals at least 3 months old, with five of six from animals more than 5 months old.

With the exception of differences in the density of axonal projections to layer 4B and the laminar specificity of infragranular projections, five of six layer 4Cα neurons have similar laminar patterns of axonal arborization. These five neurons also have in common the restriction of their dendritic branches predominantly to layer 4Cα (Figs. 3 and 4b–4c). In some cases the dendritic arbors appear to be asymmetric, to avoid crossing into layer 4Cβ (Figs. 3c and 4c). The sixth cell has branches that cross the middle of layer 4C (Fig. 4a).

All six cells have axonal projections to layer 3B, but only four have strong projections to layer 4B (Figs. 3 and 4a; see Figs. 4b–4c for cells that do not project heavily to 4B). All six neurons also have descending axons that extend into layer 6 and branch in infragranular layers, but all end in the plane of the slice without entering the white matter. Axonal branches in the infragranular layers can be restricted to layer 5 (Figs. 3c and 4b) or layer 6 (Fig. 4c), or extend into both layers (Figs. 3a–3b). When projections are present in layer 6 they are relatively sparse and do not appear to be specific for the upper or lower half of the layer (Figs. 3a–3b and 4c).

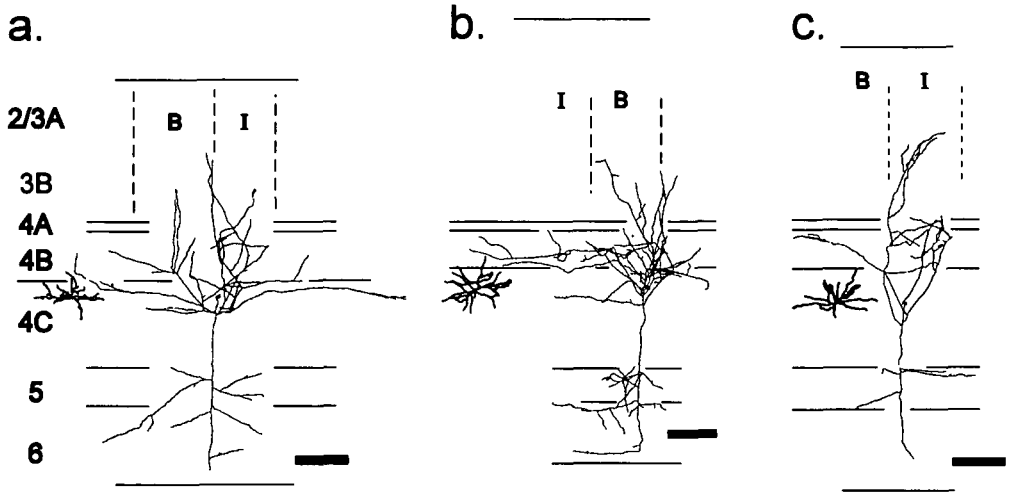

Fig. 3. Camera lucida reconstructions of layer 4Cα spiny stellate neurons. All three neurons (a-c) project axonal branches to layers 3B, 4B, and 5. In addition, the neurons shown in (a) and (b) have axonal branches in layers 6 and 4Cα but most of the 4Cα branches extend upward into 4B. The cells illustrated in (a) and (b) both project to blobs and interblobs in layer 3B, while the cell in (c) projects just to an interblob. None of these cells has axonal branches in layer 4Cβ and none project to the white matter. The dendritic arbors of these cells are restricted to layer 4Cα and lower layer 4B. This is the case for the neuron shown in (c), despite the positioning of its cell body near the middle of layer 4C. See legend of Fig. 2 for conventions. Scale bars = 200 μm.

The neuron with dendrites crossing mid-4C is unique in that it projects axons strongly and specifically to layer 5A (Fig. 4a). This neuron also focuses its projection within layer 4C onto the middle of the layer, while the other five cells have projections of varying density confined to layer 4Cα. Finally, this neuron is also unique in that its projection to layer 4B is confined to the upper half of the layer. Thus, there is a distinct absence of projections to the zone in upper 4Cα/lower 4B that contains the dendrites of upper layer 4Cα spiny stellates (Fig. 3b, see Mates & Lund, 1983).

Thus, layer 4C spiny stellates with dendrites that span the middle of layer 4C may contribute uniquely to the local circuitry

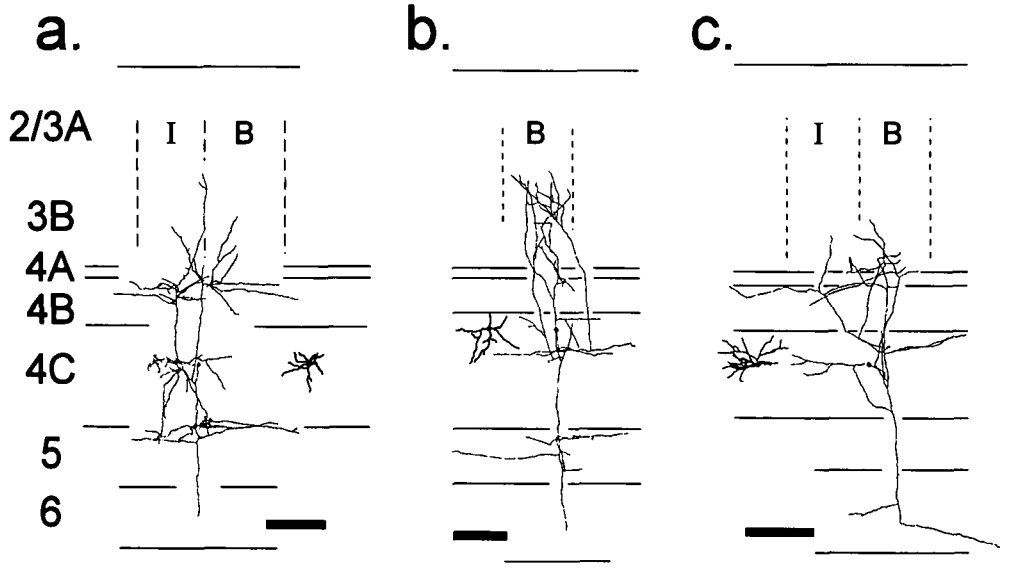

Fig. 4. Camera lucida reconstructions of three layer 4Cα spiny stellate neurons. These neurons have axonal arbors in layers 3B and 4C, but either project less heavily to layer 4B than those shown in Fig. 3 (b,c) or their layer 4B projections are restricted to the upper part of the layer (a). All three neurons have axonal branches in their layer of origin, but the projections of the neuron in (a) are restricted to the middle of layer 4C. This cell also has a dense projection to layer 5A. Note that the dendritic arbor of this neuron (a) also spans the middle of layer 4C, while the dendrites of the others are restricted to layer 4Cα. Axonal projections to layer 3B are to both blob and interblob compartments for (a) and (c) and are blob specific for the neuron in (b). The cell illustrated in (b) has axonal branches throughout layer 5 but not layer 6. The neuron in (c) has axonal branches in layer 6, but not 5. Scale bars = 200 μm.

in V1, perhaps related to the likelihood that they receive strong input from both M and P geniculate afferents (Mates & Lund, 1983; Blasdel & Fitzpatrick, 1984). However, not all spiny stellates in the middle of layer 4C fall into this category since some have asymmetric dendritic arbors that do not cross the middle of 4C (Figs. 3c and 4c).

Finally, it is important to consider the possibility that projections from layer 4Cα spiny stellate neurons specifically target either blob or interblob regions within layer 3B. Of the six neurons in our sample, four clearly form at least part of their axonal arbor within both blob and interblob regions (Figs. 3a-3b, 4a, and 4c). Of the remaining two, one projects exclusively to a blob (Fig. 4b) and the other exclusively to an interblob (Fig. 3c). Of the four neurons that project to both a blob and an interblob, two are situated under a blob/interblob transition and have roughly equal projections to the overlying blob and interblob (Figs. 3a and 4a). The other two are located under a blob and project predominantly to their overlying blob (Figs. 3b and 4c). The neuron projecting specifically to a blob has its soma under that blob (Fig. 4b), while the neuron projecting only to an interblob has its soma under that interblob region (Fig. 3c). Nevertheless, axons of the blob-specific neuron appear to "avoid" the interblob region while those of the interblob-specific cell curve away from the nearest blob. Also, the projection of the interblob-specific neuron to layer 4B is specific for regions beneath interblobs (Fig. 3c). These observations suggest the possibility of specific cell classes that are either blob-specific, interblob-specific, or nonspecific.

Layer 4B pyramidal and spiny stellate neurons

We labeled 15 spiny neurons with cell bodies in layer 4B. One third ($n = 5$) have a spiny stellate morphology (Fig. 5a) and two thirds ($n = 10$) have a pyramidal morphology (Figs. 5b, 6a, and 6b). We did not note any systematic difference in axonal morphology between pyramidal and spiny stellate neurons. We also did not note any differences between layer 4B neurons with somata at different depths within the layer or at different positions relative to the overlying blob and interblob regions.

As a population, layer 4B spiny neurons contribute very widespread clustered axonal branches to layers 4B and 5B (Figs. 5b and 6a-6b). They also project laterally spreading and clustered axons throughout the depth of layer 2/3; these projections are highly specific for blob regions (Figs. 5-6). These cells also occasionally contribute axon collaterals to layer 6. It appears that virtually all of the spiny neurons in layer 4B project to the white matter. Our analysis reveals that five of six pyramidal neurons project to the white matter (four were ambiguous) as do four of four spiny stellate neurons (one ambiguous).

Every one of the 15 layer 4B spiny neurons in our sample forms at least part of its axonal arbor within layer 2/3. These projections usually extend throughout the depth of layer 2/3 (12/15 cells, Figs. 5 and 6b; see Fig. 6a for counter-example) and are sometimes considerably denser in layer 2/3A than in layer 3B (5/15 cells, Fig. 5a). For all 15 cells, the projection to layer 2/3 is highly specific for blob regions, regardless of whether the soma is beneath a blob (Figs. 5a-5b) or interblob (Figs. 6a-6b). The lateral spread of axonal arbors within layer 2/3 varies from just a single blob (Fig. 6a) to three blobs (not shown). Because the axons that we can observe are limited to those which lie in the plane of the slice, we cannot determine whether the variability between neurons results from actual differences between neurons *in vivo* or from variability in the plane of slicing relative to an axis of elongation of axonal arbors. We also cannot rule out the possibility that some cells have longer lateral projections than we are able to observe. This is also important in assessing the lateral spread of the axonal arbors of these cells within layers 4B and 5, as well as other cell types (see below).

All 15 neurons in our sample also form substantial axonal arbors within layer 4B. Again the lateral spread within the layer varies considerably (compare Figs. 5a-5b to 6a) but can be as long as 2 mm. Whenever widespread arbors are present they form clear clusters spaced about 500 μm apart (see Figs. 6a and 6b). These clusters of axon collateral branches have no clear relationship to the overlying CO blobs.

These cells occasionally have very weak axonal projections to layer 4Cα (four of 15 cells; Figs. 6a-6b), but they generally have a main descending axon that passes through layer 4C without branching (except near the 4B/4Cα border where collaterals emerge that rise obliquely into layer 4B; Fig. 5a). The descending axon almost always either extends to the white matter (9/15 cells,

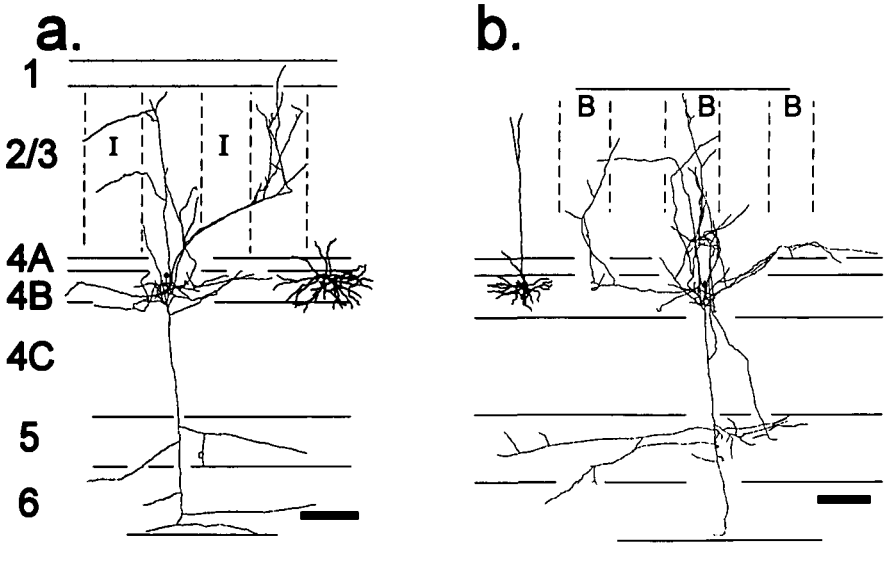

Fig. 5. Camera lucida reconstructions of layer 4B neurons with somata under CO blobs. The neuron shown in (a) is a spiny stellate neuron whereas the one in (b) is a pyramid. Both neurons project axons throughout the depth of layer 2/3, and to layers 4B and 5. The projections within layer 2/3 are highly specific for CO blobs. The neuron shown in (a) also has axonal branches in layer 6 and its layer 2/3 projection is more dense in 2/3A than 3B. See previous figures for conventions. Scale bars = 200 μm.

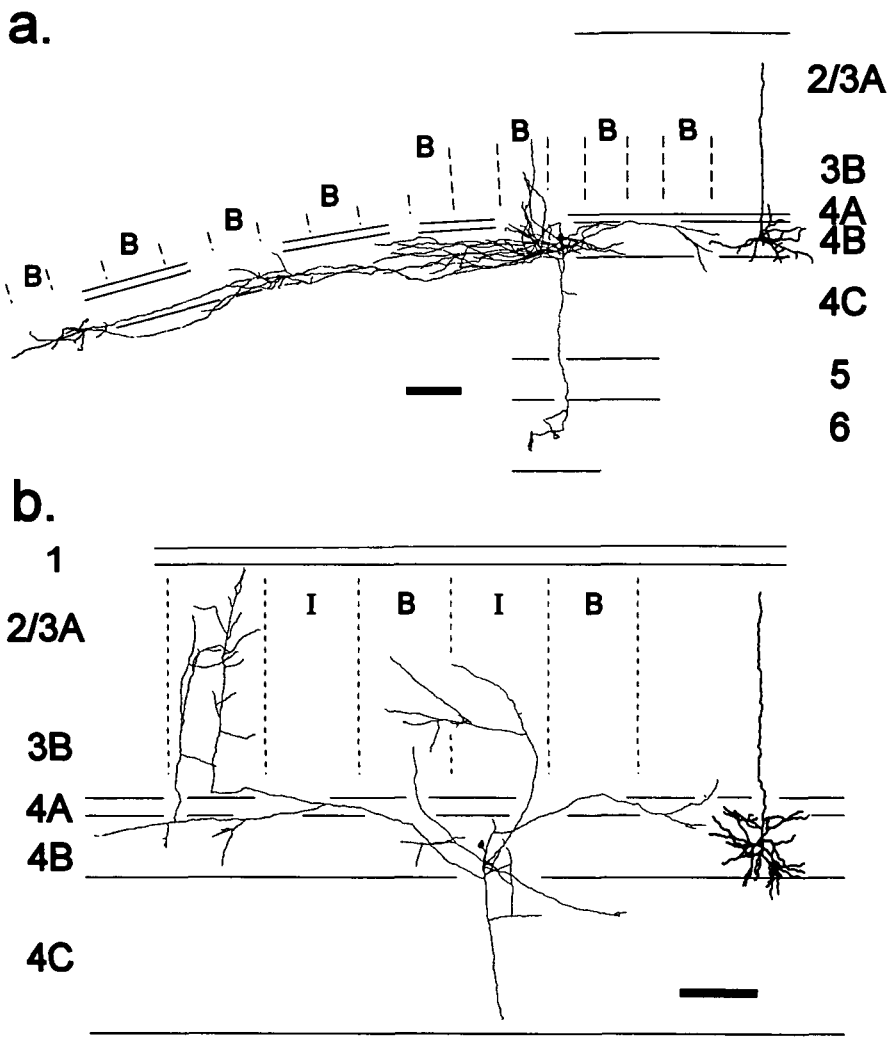

Fig. 6. Camera lucida reconstructions of layer 4B pyramids with somata under interblobs. The slanted lines in (a) indicate laminar boundaries as the tissue curves. These neurons have long-distance, clustered axonal projections in layer 4B [particularly the cell in (a)] and blob-specific projections in layer 2/3. The axons of the neuron shown in (a) do not extend above layer 3B. The neuron shown in (a) projects to layer 6 but not to the white matter. The descending axon of the neuron in (b) was cut in 4Cβ, and it is therefore not known whether it projected to the white matter. See previous figures for conventions. Scale bars = 200 μm.

Figs. 5a–5b) or leaves the plane of the slice before ending (5/15 cells, Figs. 6b). On the way, it usually gives off collaterals in layer 5 (11/12 cells, Figs. 5a–5b; the cell that does not is also the lone, confirmed nonprojecting neuron, Fig. 6a), and occasionally in layer 6 (3/12 cells, Fig. 6a; 2/12 project to both layers 5 and 6, Fig. 5a). Thus, nine of 12 cells in our sample lack a projection to layer 6, and layer 6 is therefore not a primary target of most layer 4B neurons. (Three cells are not included in the analysis of projections to layers 5 and 6 because their descending axons leave the plane of the slice in layer 4C; see Fig. 6b.)

Axonal projections within layer 5 can extend up to 1 mm laterally, particularly within layer 5B. These arbors sometimes form clusters of finer collateral branches (Fig. 5b) which are in register with those in layer 4B in the few cases where both are observed from the same cell (not shown). When axonal projections are present within layer 6 they are generally shorter and unclustered, and can be found in the upper (Fig. 6a) or lower half (Fig. 5a) of the layer.

Layer 4A pyramidal and spiny stellate neurons

We labeled five spiny neurons with somata in layer 4A. Two have a spiny stellate morphology and the remaining three have a pyramidal morphology. These cells resemble layer 4B spiny neurons in that there is no clear systematic difference in the local axonal arbors of spiny stellate versus pyramidal neurons. These neurons, however, differ from layer 4B neurons in a number of important respects. The differences that are perhaps most important functionally are related to axonal projections to layer 2/3. The projections of layer 4A cells to layer 2/3 are not blob-specific, have a more restricted lateral extent, and are restricted primarily to the bottom half of layer 2/3 (Fig. 7).

The lack of blob specificity of axonal projections from layer 4A spiny neurons is illustrated in Fig. 7. Both pyramidal (Figs. 7a and 7c) and spiny stellate (Fig. 7b) neurons project to both blob and interblob regions. Because of the limited lateral extent of axonal projections within layer 3 (typically 300–500 μm, but see Fig. 7c), these projections are generally denser to either a blob or interblob region, depending on the position of the cell body relative to the overlying blobs. For example, the neurons illustrated in Figs. 7a–7b have cell bodies beneath blobs and project more strongly to the overlying blobs than to the adjacent interblobs, while the cell illustrated in Fig. 7c is situated under an interblob and projects more strongly to the interblob than to the adjacent blob.

Layer 4A spiny neurons also differ from layer 4B neurons with respect to axonal projections to deeper layers. Axonal

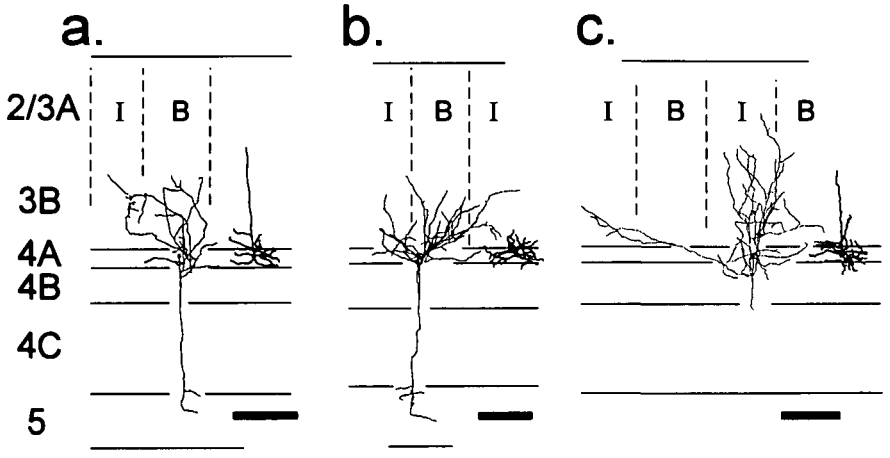

Fig. 7. Camera lucida reconstructions of layer 4A neurons. Cells shown in (a) and (c) are pyramidal neurons, while the cell illustrated in (b) is a spiny stellate neuron. These neurons project axons predominantly to layer 3B [the neuron in (c) also has a few axonal branches in layer 2/3A] and this projection is not specific for blobs or interblobs. These cells also project axonal branches to their own layer (4A) and branch in layer 5 (a, b). The neurons in (a) and (b) are nonprojection cells and the neuron in (c) is ambiguous. See previous figures for conventions. Scale bars = 200 μm.

branches that emerge from the main descending axon in layer 4B usually rise up to layer 4A without branching, and all have branches emerging in layer 4A (Fig. 7). The projections within layer 4A are comparable in extent to those in layer 3 (300–500 μm). One of the two spiny stellate neurons has several axonal branches in layer 4Cα (not shown), but the remaining cells all lack axonal branches in layer 4C. All of the cells whose descending axon does not leave the plane of the slice before entering layer 5 (3/3 cells) have axonal branches in layer 5 (Figs. 7a–7b). The lateral extent of these projections is restricted to just 150 μm or less. Only two of the five cells can be unambiguously classified as projecting versus nonprojecting; one is a pyramidal neuron (Fig. 7a) and the other a spiny stellate (Fig. 7b), and both lack an axonal projection to the white matter. In addition, the descending axons of both cells end within layer 5 and do not extend into layer 6. Thus, we did not observe any part of the axonal arbor in layer 6 for any of the neurons in our sample.

Layer 2/3 pyramidal neurons

Pyramidal neurons with cell bodies in layer 2/3 are divided into two groups: those with somata in layer 3B and those in layer 2/3A. We labeled nine pyramidal neurons with cell bodies in layer 2/3A and eight with cell bodies in layer 3B.

Comparisons of layer 2/3A (Fig. 9) versus layer 3B pyramidal neurons (Fig. 8) reveal similarities in terms of the specificity of their axonal arbors within layer 2/3 for blobs versus interblobs; the laminar specificity of their axonal projections to deeper layers (4A–6); and the proportion of neurons projecting to the white matter. These cells differ, however, in that layer 3B neurons project axons to layers 2/3A and 3B (8/8 cells), while layer 2/3A

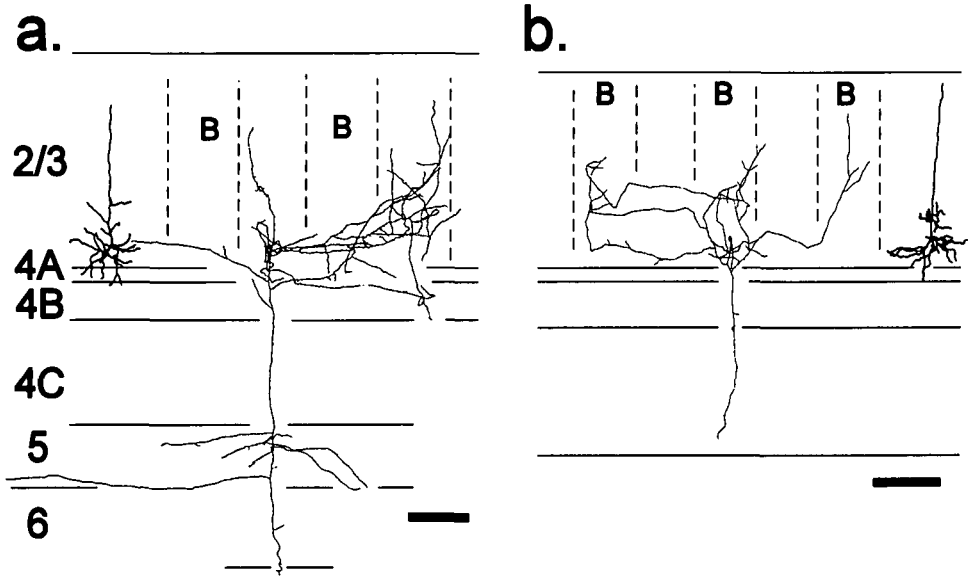

Fig. 8. Camera lucida reconstructions of layer 3B pyramidal neurons. These cells project blob-specific axons in layer 2/3: if the cell body is in an interblob, the projection is interblob specific (a); if the cell body is in a blob, the projection is blob specific (b). These cells also have a descending axon that branches sparsely in layer 4B and more densely in layer 5 (a). The axon of the neuron shown in (b) was cut off in layer 4C. The neuron in (a) is a projection neuron. See previous figures for conventions. Scale bars = 200 μm.

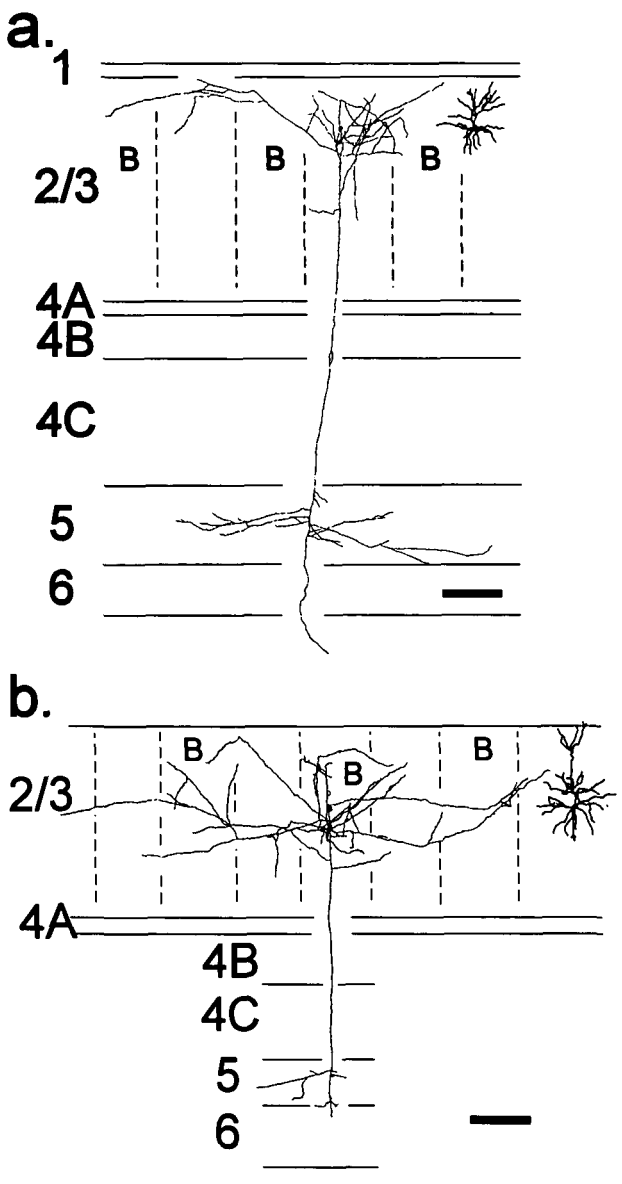

Fig. 9. Camera lucida reconstructions of layer 2/3A pyramidal neurons. Like layer 3B pyramidal neurons, the axonal branches of layer 2/3A blob neurons target blobs (b) and interblob neurons target interblobs (a). However, these neurons do not project axons to layer 3B. The descending axon of each cell branches in layer 5 but not in layer 6. The cell in (a) is a projection neuron. See previous figures for conventions. Scale bars = 200 μm.

neurons restrict their layer 2/3 projection to layer 2/3A (9/9 cells).

We will first describe in detail the characteristics that are common to both layer 2/3A and layer 3B pyramidal neurons. As expected from previous studies (Livingstone & Hubel, 1984, McGuire et al., 1991), the axonal arbors within layer 2/3 are blob specific; neurons with cell bodies in blob regions project axons more heavily to blobs (Figs. 8b and 9b), while those in interblobs project predominantly to interblobs (Figs. 8a and 9a). Typical levels of blob specificity for blob and interblob neurons are shown in Figs. 8–9. The neuron illustrated in Fig. 9b is an example of the least specific projections observed. There is specificity for blob versus interblob regions, but it is not perfect.

Layer 2/3A and layer 3B pyramidal neurons are also similar in terms of their deeper axonal projections. Only one cell, a layer 3B pyramidal neuron, lacks a projection to deeper layers. The descending axon of five of nine layer 2/3A neurons forms at least one branch in layer 4B as do five of eight layer 3B neurons. These projections are typically very sparse, with just one unbranched axon collateral emerging in layer 4B (see Figs. 8b and 9a), but sometimes secondary branches are present within the layer (Fig. 8a). Blob neurons are no more or less likely than interblob neurons to form such branches; six of ten blob neurons have axonal branches in layer 4B, as do four of seven interblob neurons.

With the exception of the layer 3B neuron that lacks a descending projection, all of the layer 2/3 neurons whose descending axon does not leave the plane of the slice above layer 5 have collateral branches in layer 5 (13/14 cells). These projections are typically most extensive in layer 5B. There are generally not enough secondary branches in this layer to determine whether the projection is specific for regions under CO blobs or interblobs. However, two neurons do form clear clusters of axonal branches in layer 5 (not shown). For both cells, these are directly under axon clusters that are present in layer 2/3. For the blob neuron they are blob specific and for the interblob neuron they are interblob specific. In general, however, the specificity is not as great as within layer 2/3 (Figs. 8a and 9a).

Of the nine layer 2/3A pyramidal neurons, three of six project to the white matter (three do not), while the remaining three have descending axons that leave the plane of the slice, precluding characterization. Roughly the same proportion of layer 3B neurons project to the white matter (three of five, three ambiguous).

Although a total of six layer 2/3 neurons clearly project to the white matter, only one forms an axonal branch in layer 6, and this is a single short branch (Fig. 8a). In addition, another five neurons that clearly lack a projection to the white matter also lack a projection to layer 6. The remaining six layer 2/3 pyramidal neurons cannot be characterized in this regard because the descending axon leaves the slice above or within layer 6.

Layer 5 spiny neurons

Our sample includes 16 spiny neurons with cell bodies in layer 5. Although most of these have a clear pyramidal morphology, two of these lack a distinct, elongated apical dendrite (Fig. 10a). From a functional standpoint, however, this morphology is probably not very different from pyramidal neurons which have apical dendrites of varying lengths, generally lacking branches outside of layer 5 (Figs. 10–13). Most of these have a very short, fine apical dendrite that extends into the bottom of layer 4Cβ (see Figs. 11b and 12a–12b), while some have longer apical dendrites extending as high as layer 2/3A (Figs. 10b and 13a). These morphologies appear to represent a continuum, with neurons lacking an obvious apical dendrite at one extreme and those with apical dendrites extending to layer 2/3A at the other. We have noted no correlation between the length of apical dendrites and patterns of axonal arborization within this group of cells. We have not observed layer 5 neurons with large cell bodies and

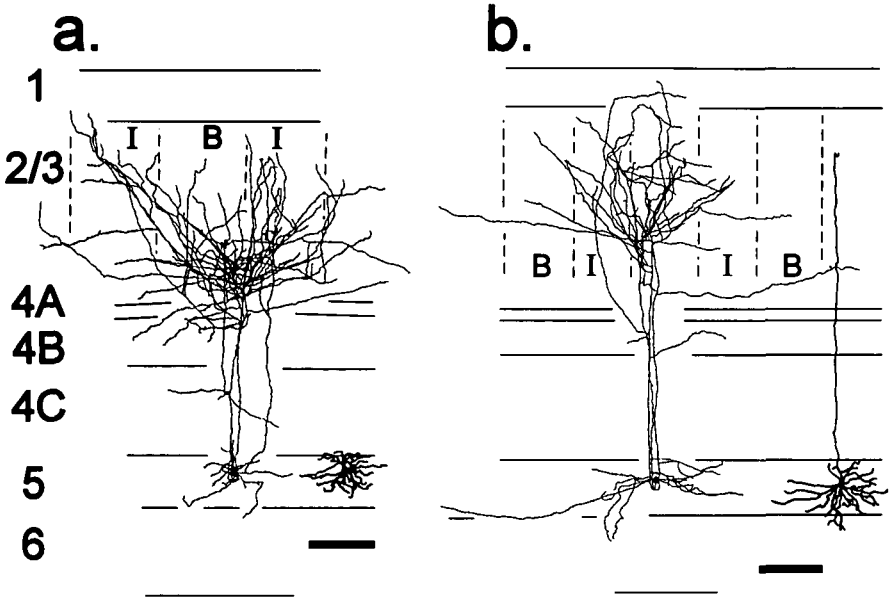

Fig. 10. Camera lucida reconstructions of layer 5 spiny neurons with dense axonal projections in layer 2/3. The neuron illustrated in (a) has no distinct apical dendrite, while the neuron in (b) has an obvious pyramidal morphology with an apical dendrite extending into layer 2/3. These cells project axons most heavily to layer 2/3 without any specificity for CO blobs or interblobs. The neuron in (b) has heavier axonal projections to layer 2/3A than to layer 3B. Both cells have occasional axonal branches in layer 4B and in the case of the neuron shown in (a), a few branches in layer 4C. They both project axons to their own layer, with some unbranched collaterals extending into layer 6. These are nonprojection neurons. See previous figures for conventions. Scale bar = 200 μm.

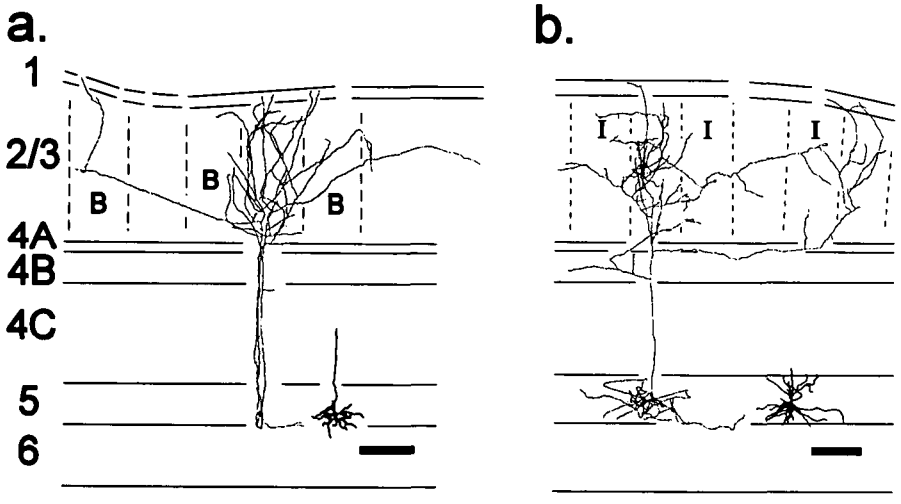

Fig. 11. Camera lucida reconstructions of layer 5 neurons. These two neurons have a pyramidal morphology with a short apical dendrite [especially short in case (b)]. Their densest axonal projections are in layer 2/3. These cells both project clusters of axonal branches in layer 2/3. In (b), the clusters are in two blobs, but projections are more sparse in an intervening blob. (This observation suggests the possibility of ocular dominance rather than blob specificity. See Results.) The neuron shown in (b) has limited axonal branching in layers 4A and 4B and heavier branching in layer 5, while the neuron in (a) has few branches outside layer 2/3. See previous figures for conventions. Scale bars = 200 μm.

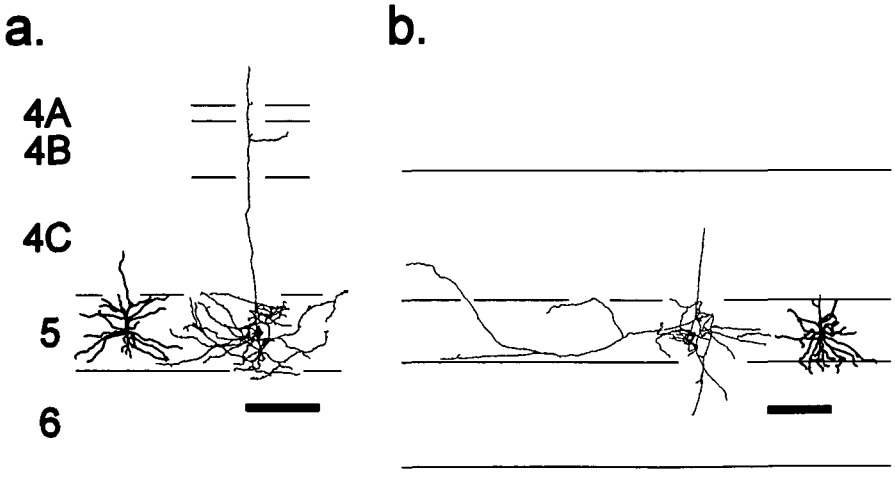

Fig. 12. Camera lucida reconstructions of layer 5 spiny neurons. Both neurons have a pyramidal morphology with a short apical dendrite [especially short in case (b)]. Unlike most layer 5 spiny neurons, these cells do not project dense axonal branches into layer 2/3; their main projection is to layer 5. These cells do not project to the white matter. The ascending axon of the neuron shown in (a) has a branch in layer 4B and ends unbranched in layer 3B. For the neuron illustrated in (b), axonal branches do not extend beyond the middle of layer 4C. See previous figures for conventions. Scale bars = 200 μm.

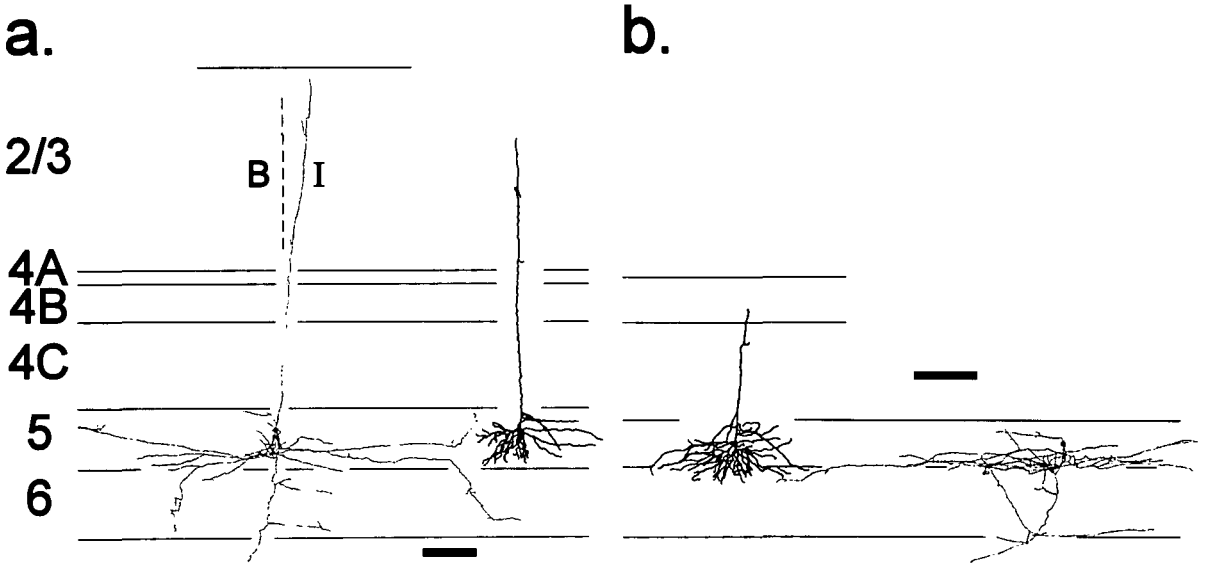

Fig. 13. Camera lucida reconstructions of layer 5 projection neurons. These neurons have a "backbranching", pyramidal dendritic morphology; apical dendritic branches arc downward. Backbranching is particularly pronounced in (b). The neuron illustrated in (b) does not project axons to superficial layers while in (a) only one ascending axon projects to layer 2/3. Instead, these neurons have lateral axonal projections in layer 5 and sparse, clustered projections to layer 6. A photograph of the neuron illustrated in (b) is shown in Fig. 1c. See previous figures for conventions. Scale bar = 200 μm.

long apical dendrites that form a tuft in layer 1 (see Lund & Boothe, 1975; Valverde, 1985).

We did, however, label three neurons with a distinctly different pattern of dendritic arborization. These neurons have very dense and widely spreading basal dendrites, and branches off the apical dendrite that arc downward ("backbranching"). The backbranching dendrites also extend long distances laterally. This morphology is most distinct in two of these neurons, of which one is illustrated in Figs. 1c and 13b. The third neuron of this type has a backbranching dendrite but the arbor does not extend as far laterally (Fig. 13a). This pattern of dendritic arborization is correlated with a distinct pattern of axonal arborization (see below).

Although the majority of layer 5 spiny neurons in our sample cannot be separated into distinct groups based on their patterns of dendritic arborization, they do seem to fall into two groups on the basis of patterns of axonal arborization. Nine of 16 cells form extremely dense axonal arbors within layer 2/3 (Figs. 10–11), while the remaining seven lack a strong axonal projection to layer 2/3 (Figs. 12–13). All three "backbranching" cells fall into the latter group.

Cells projecting densely to layer 2/3 have recurrent axon collaterals that curve upward not far below the cell body (Figs. 10–11). Laterally spreading axonal branches emerge as side branches from these rising collaterals. These side branches are found in layers 2/3 (9/9 cells), 4B (9/9 cells), and 5 (8/9 cells), and rarely in layers 4A (2/9 cells) or 4Cα (1/9 cells, see Fig. 10a). Secondary branches arising from layer 5 side branches occasionally extend into layer 6, but they never form branches in layer 6. None of these cells (0/9) have a descending axon extending into the white matter.

The axonal projections from these cells into layer 2/3 are the most dense of all of the projections we have observed. These projections are sometimes considerably stronger to layer 2/3A than to layer 3B (3/9 cells; Figs. 10b and 11b). They are usually not specific for blob versus interblob regions (Figs. 10 and 11a). Neurons with cell bodies beneath blob regions (6/9) and interblob regions (3/9) project heavily to both blobs and interblobs in layer 2/3. Three neurons do, however, have clearly clustered axonal arbors within layer 2/3 that have some preference for blob regions (Fig. 11b). The specificity for blobs is clearly far from perfect, as even the neuron in Fig. 11b, which is the most specific in our sample, has numerous axon collateral branches in interblob regions. The other two neurons displaying blob specificity have axonal arbors similar to that shown in Fig. 11b, in that they appear to skip over a blob adjacent to the one directly over the cell body. However, the neuron shown in Fig. 11a also skips over one blob to target a more distant blob even though its soma is beneath an interblob and it projects heavily to the overlying interblob region. This observation suggests that the axonal clustering we observe may actually reflect specificity for some other aspect of columnar organization that is related to blobs, such as ocular dominance columns. The axonal projections within layer 4B are considerably weaker than those in layer 2/3 (Figs. 10 and 11b). They typically consist of 1–3 branches emerging from a rising collateral (Figs. 10b and 11b), or branches from layer 3B that dip back into layer 4B (Fig. 10a). Axonal branches in layers 4A and 4Cα are also sparse in the few cells that have them (Figs. 10a and 11a).

Axonal projections of cells that project heavily to layer 2/3 vary considerably in the density and extent of their projections to layer 5. But their layer 5 projections are typically weaker than those from cells that do not project heavily to layer 2/3 (see below). At the extremes, one cell lacks axonal branches in layer 5 (not shown, but see Fig. 11a for a cell with just one branch), while others have long collaterals in layer 5B (Fig. 10b). More typically, the axon collaterals in layer 5 are found no further than 300 μm from the cell body.

Other layer 5 neurons lack dense axonal projections to layer 2/3 (Figs. 12–13). Instead these cells form their densest axonal

arbors in layer 5 where they can extend up to 900 μm laterally, particularly in layer 5B (Figs. 12b and 13). The arbors within layer 5 are, however, not always extensive (see Fig. 12a). In addition, none of the nine cells projecting densely to layer 2/3 projects to the white matter, while three of the remaining seven do. Interestingly, all three projection neurons are the "backbranching" cells described above (Fig. 13). All of these cells also have axonal branches in layer 6 (no other layer 5 cells do) and have very long collaterals in layer 5B (Fig. 13). The projections to layer 6 are relatively weak, but highly focused, forming discrete clusters beneath the cell body (Fig. 13b) or further laterally (Fig. 13a). Because the layer 5 projection neurons have axonal and dendritic morphologies that are distinctly different from nonprojecting neurons, we consider them to be a distinct cell type that is likely to contribute uniquely to computations within V1 and in its extrinsic targets.

Discussion

Summary

By reconstructing the axonal and dendritic arbors of intracellularly labeled spiny neurons in macaque V1, we have been able to identify potential sources of local excitatory input to neurons that project to the extrastriate cortex. The method allows axonal projections to be unequivocally linked to their parent neurons. Nevertheless, our results have clear limitations that must be carefully considered in assessing the actual patterns of connectivity that are likely to be present.

We provide evidence that the M and P pathways converge onto neurons in both the blob and interblob regions of layer 3B at the earliest stage of local processing; spiny stellate neurons in both the M and P recipient layers, 4Cα and 4Cβ, respectively, project directly to both blobs and interblobs. Layer 4A neurons also project to both blobs and interblobs in layer 3. But the axonal projections of layer 4B neurons are highly specific for blobs in layer 2/3, suggesting a relatively strong M-stream contribution. Layer 5 neurons are also likely to contribute to considerable mixing of the M and P pathways because they can project heavily to layers 2–4B without any apparent specificity for blobs or interblobs.

These results must be carefully scrutinized as they relate to results from previous studies using different methods. Taken together, the discrepancies and consistencies between studies provide greater insight into patterns of connectivity than can be gleaned from any single study.

Technical considerations

Before discussing our results in detail, it is useful to discuss technical advantages and limitations of the method we have used. We are confident that all of the axonal and dendritic processes of the neurons in our sample were detected, in so far as they were present in the plane of their parent brain slices. Thus, all of the projections that we observed exist and arise from the cells we identified. We cannot rule out the possibility of additional projections or cell types we did not detect. But we have generally obtained a large enough sample of spiny neurons from each layer that we are confident that only rare cell types and axonal projections from a given layer were missed, with the following exceptions.

Our sample of neurons in layer 4C is limited. We have labeled only three spiny stellate neurons from layer 4Cβ. Several intracellularly labeled, layer 4Cβ spiny stellates have been described previously (Katz et al., 1989, Anderson et al., 1993); these studies clearly reveal cell types missed in our sample, particularly neurons that project to infragranular layers.

Similarly, our sample of six layer 4Cα spiny stellates is adequate to provide information about projections to blobs versus interblobs in layer 3B (see below), but probably does not represent all cell types from this layer. Of the six cells in our sample, several are unique in their patterns of axonal arborization, suggesting that still more varieties would be observed if the sample size were increased. Indeed, three intracellularly labeled 4Cα spiny stellates described previously are all different from any we sampled (Katz et al., 1989; Anderson et al., 1993).

We also missed at least one relatively rare type of layer 5 pyramidal neuron. Golgi studies have revealed layer 5 pyramidal neurons with large cell bodies and apical dendrites that extend to layer 1, where they form a "tuft" of dendritic branches (Lund & Boothe, 1975, their plate 3; Valverde, 1985, his Fig. 24). Despite the large number of layer 5 spiny neurons in our sample, we did not label a cell with this morphology.

Otherwise, our repeated observations of the same types of spiny neurons within the various layers suggest that our sample sizes are large enough to represent most neuron types. In further support of this notion, the combined projection patterns of neurons we labeled are adequate to describe the projections observed following extracellular tracer injections (Blasdel et al., 1985; Fitzpatrick et al., 1985, Yoshioka et al., 1994). Nevertheless, we cannot rule out the possibility that we missed rare neuron types, or cells that are difficult to record from using patch electrodes and whole-cell methods.

It is also important to consider the young ages of the animals used in this study; only one cell is from an animal more than 9 months old. However, 45 of the 62 neurons are from animals more than 5 months old and all but four are from animals at least 3 months old. Three of the four cells from younger animals are layer 4Cβ spiny stellates; no other layer 4Cβ spiny stellates were observed. Otherwise, all of the neuronal types we identified were observed in both the 3–5 month and >5 month age groups. Amongst these neurons we did not detect any difference between the cells from the older versus younger group. In view of evidence that laminar specificity of axonal arbors, ocular dominance columns, and specificity of circuitry for CO blobs all develop prenatally in macaque V1 (Lund et al., 1977; Callaway, 1993; Horton & Hocking, 1996), we feel that, with the exception of layer 4Cβ spiny stellates, the neurons we have studied are representative of those in mature animals.

Convergence of functional streams by V1 local circuits

Because our material was double stained for CO and biocytin, we were able to assess patterns of axonal projections relative to CO blobs and interblobs in layer 2/3. These observations are useful for understanding the contributions of the M and P streams to the extrastriate projection neurons in layers 2–4B of V1. In particular, we were interested in the direct and indirect transfer of information from the M and P recipient layers, 4Cα and 4Cβ, respectively, to neurons in layer 4B and to the CO blobs and interblobs of layer 2/3.

Projections from layer 4

Functional studies have revealed that neurons in both CO blob and interblob regions can be activated by visual stimulation even after inactivation of M or P layers of the LGN (Nealey & Maunsell, 1994). Thus, there is convergence of M and P input onto these neurons. It is less clear, however, what anatomical substrates mediate this convergence. Lachica et al. (1992) report that neurons in layer 3B blobs receive convergent input from both M and P streams relayed directly by layers 4Cα and 4Cβ, respectively, but that interblobs do not receive M input either directly from layer 4Cα or less directly from layer 4B. Yoshioka et al. (1994) on the other hand argue that only interblobs receive direct input from layer 4C and that this input already provides mixed M and P information because it derives from neurons in mid-4C that receive input from both M and P geniculate afferents. They suggest that input to the blobs is also convergent but less direct, originating from the top and bottom of layer 4C and relayed through layers 4B and 4A, respectively. In this scheme layers 4A and 4B do not contribute input to interblobs.

Although our observations do not resolve these issues, they do provide important new insight. Our results suggest that neither interpretation is entirely correct. We further suggest that differences between studies might reflect functional differences between blobs. In our discussion here we do not intend to fully explore all of the possible explanations for differences between studies, rather we will focus on the following issues as they relate to our findings: (1) the points on which all studies are in agreement; (2) points of disagreement between studies about which our findings provide new insights; and (3) points that will require further studies for clarification (2 and 3 are not necessarily distinct categories). This discussion will focus on the reports of Lachica et al. (1992), Yoshioka et al. (1994), and the present findings because these studies have combined labeling of intrinsic circuitry with CO staining to reveal blobs.

It is generally agreed that axonal projections to layer 4B arise from layer 4Cα but not 4Cβ, and that layer 4B spiny neurons project strongly and specifically to blobs in layer 2/3. Blobs therefore receive substantial M input *via* this pathway. Furthermore, our results show that the blob-specific projections from layer 4B arise from both spiny stellate and pyramidal neurons. It is also agreed that layer 4A receives stronger input from layer 4Cβ than 4Cα. Lastly, it is agreed that interblobs receive input from layer 4Cβ and that blobs receive input from layer 4A. But whether the projections from layer 4Cβ or 4A are specific for blobs versus interblobs is more controversial.

Our findings agree with Lachica et al. (1992) that neurons in both layers 4Cβ and 4A project to both blobs and interblobs. Yoshioka et al. (1994) however, report interblob-specific projections from layer 4Cβ and blob-specific projections from layer 4A. We feel that our findings rule out the possibility that all layer 4A neurons project specifically to blobs and support the conclusion of Lachica et al. (1992). Nevertheless, it is possible that some blobs might be functionally different from others (see below) and in view of the small samples in all of these studies it is possible that some layer 4A neurons might make blob-specific projections and/or some interblobs may lack layer 4A input.

Our findings provide less insight into the specificity of projections from layer 4Cβ because our sample is small and the newborn cells might not be representative of mature neurons. The cells in our sample however, clearly project to blobs, and combined with the evidence of Lachica et al. (1992) it appears likely that layer 4Cβ spiny stellates do project to blobs as well as interblobs. On the other hand, Yoshioka et al. (1994) clearly show anterograde label from a layer 4Cβ injection that avoids a blob to specifically target an interblob. But they only report on one layer 4Cβ injection. Therefore, we suggest that the likely resolution of these differences will again be related to possible functional differences between blobs. Perhaps most blobs receive 4Cβ input, but some do not.

We find layer 4Cα spiny stellates that project to both blobs and interblobs in layer 2/3. But Lachica et al. (1992) report that only blobs receive input from this layer. Although we clearly see projections to interblobs (see Figs. 3–4), these are not particularly dense and the overall density of blob versus interblob inputs cannot be revealed by our small sample of intracellularly labeled neurons. We therefore favor the interpretation that the densest projections are to blobs and that the retrograde labeling method used by Lachica et al. (1992) was not sensitive enough to detect the weaker projection to interblobs. Another possibility, however, is that some interblob regions are functionally different than others and truly lack input from layer 4Cα. This possibility is suggested by the observation of blob-specific as well as interblob-specific layer 4Cα spiny stellates (Figs. 3c and 4b).

Anatomical studies have contributed enormously to our understanding of local circuits in V1. However, we feel that resolution of the precise patterns of connectivity will require the incorporation of functional analyses. For example, despite the clear agreement that layer 4B receives *anatomical* input from layer 4Cα and not 4Cβ, studies using "photostimulation" have revealed that layer 4B pyramidal neurons receive substantial *functional* input from layer 4Cβ, presumably onto their apical dendrites (Sawatari & Callaway, 1996). Similarly, demonstrations of specific projections to blobs or interblobs in layer 2/3 may not reflect functional selectivity. For example, dendrites of layer 2/3 neurons freely cross blob/interblob transitions (Hubener & Bolz, 1992) and thus interblob neurons might receive connections from the blob-specific axonal projections of layer 4B cells.

We have also alluded to the possibility of functionally specialized blob and/or interblob regions. Although there is no compelling evidence for such specialization, the possibility serves as an explanation for different results observed in anatomical studies. This possibility is also suggested by Casagrande and colleagues' observations of the anatomy of local circuits in nocturnal versus diurnal primates (see Casagrande & Kaas, 1995 for review). Perhaps the relatively strong 4Cα input to interblobs in nocturnal species reflects specialization for analyses that occur in only a minority of interblob regions in the diurnal macaque. These issues might be addressed by combining optical imaging methods to identify functionally distinct compartments with anatomical analyses to identify the sources of local input to these compartments.

Projections from layer 5

Layer 5 spiny neurons also provide considerable opportunity for convergence of M and P information onto the output neurons in layers 2–4B. First, layer 5 neurons themselves can potentially receive convergent input from any of four compartments in layers 2–4B (blobs, interblobs, 4A, 4B). Virtually all of the spiny neurons in layers 2/3 (13/14 cells) and 4B (11/12

cells) have strong projections to layer 5, regardless of their positions relative to CO blobs (but individual layer 5 neurons might not receive direct input from both blobs and interblobs). In addition, layer 4A neurons provide weaker input to this layer. Finally, most layer 5 neurons provide strong, recurrent excitatory input to layers 2–4B, with little or no preference for blobs versus interblobs. Thus, layer 5 neurons are likely to provide input arising from both the M and P streams to layer 4B and both blobs and interblobs in layer 2/3.

Interlaminar projections

The results presented here provide information about laminar patterns of information flow, from LGN recipient layers to output neurons in other layers of the primary visual cortex. As noted previously (Anderson et al., 1993), the general pattern of information flow suggested by anatomical observations in the macaque primary visual cortex appears similar to that in the cat (Gilbert, 1983; Martin & Whitteridge, 1984). Gilbert (1983) proposed that LGN input to layer 4 is fed next to layer 2/3, and then from layer 2/3 to 5. Finally, layer 5 neurons project heavily and over long distances laterally within layer 6, while the recipient layer 6 neurons project back to layer 4.

As expected, we found that in macaque V1, layer 4C projects to more superficial layers, which in turn project to layer 5. It is striking, however, that a strong layer 5 to layer 6 projection comparable to that in the cat is not detected in the macaque. The absence of such a projection does not imply, however, that layer 5 neurons cannot connect to layer 6 neurons. Macaque layer 5 pyramidal neurons make substantial long-distance projections within layer 5B (see Results). This layer contains extensive dendritic branches from a class of cells that comprises about half of the population of layer 6 pyramidal neurons (Wiser & Callaway, 1996). The remaining layer 6 neurons lack dendritic branches in this layer. Thus, the limitation of long-distance collaterals to layer 5B provides a potential means by which one class of layer 6 neurons can be specifically targeted. We propose that this organization is important for generating distinct receptive-field properties that are appropriate to the functional roles of different classes of layer 6 neurons (see Wiser & Callaway, 1996, for further details).

The absence of a strong projection from layer 5 to layer 6 raises the question: what is the primary source of input to the basal dendrites of layer 6 neurons? We find that intrinsic projections from most layers to layer 6 are either weak (from layers 4B, 4C, and 5) or virtually absent (from layer 2/3). The only strong intrinsic input arises from the layer 6 neurons themselves (Wiser & Callaway, 1996). Thus, it appears that the strongest inputs to the basal dendrites of layer 6 cells are likely to come from layer 6. The sources of input to apical dendrites are likely to vary considerably between layer 6 neurons, depending on their patterns of dendritic arborization (see Wiser & Callaway, 1996).

Our finding that only a small proportion of layer 4B neurons provide input to layer 6 differs from Golgi (Lund & Boothe, 1975) and intracellular labeling studies (Anderson et al., 1993). Results from extracellular tracer injections are, however, more consistent with the results from our larger population of layer 4B neurons. Anterograde labeling following injections in layer 4B is most extensive in layer 5 (Blasdel et al., 1985; Yoshioka et al., 1994). Thus, we suggest that the high proportions of layer 6-projecting neurons in previous Golgi and intracellular studies are simply reflective of small samples.

Lachica et al. (1992) suggested that layer 2/3A "is removed one step further than layer 3B from primary LGN input." Our results confirm that neurons in layer 4C do not project axons above layer 3B, while the neurons they target in layers 4B and 3B can project throughout the depth of layer 2/3. In addition, we find layer 4A spiny neurons that also restrict their superficial projections to lower layer 2/3. Since these neurons can receive direct geniculate input, this observation provides further support for the hypothesis. However, layer 6 pyramidal neurons, which presumably also receive direct LGN input, can project to layer 2/3A (Wiser & Callaway, 1996).

Further segregation of information flow is evidenced by our finding that none of the pyramidal neurons in layer 2/3A project axons to layer 3B. This observation suggests that it may be important for activity patterns emerging in layer 2/3A *not* to feed back to layer 3B. The predominance of axonal arbors of some layer 4B and layer 5 neurons in layer 2/3A relative to layer 3B may serve a related purpose. However, our finding that layer 3B neurons are just as likely as those in layer 2/3A to project to the white matter suggests that any additional processing in layer 2/3A is not a necessary prelude to the transfer of information to the extrastriate cortical areas.

Layer 4B contains spiny stellate as well as pyramidal neurons and the pyramidal neurons in layer 5 vary considerably in the length of their apical dendrites. However, we do not note any correlations between the different patterns of dendritic arborization and axonal arbors. This was somewhat surprising since differing patterns of dendritic arborization are likely to reflect different sources of functional input. In turn, cells with different sources of input may be expected to have different functional properties and should therefore provide outputs to different intrinsic targets. This does not appear to be the case for spiny stellate versus pyramidal neurons. However, layer 4B spiny stellates in macaque V1 might receive less input from layer 4Cβ than pyramidal neurons (Sawatari & Callaway, 1996) and perhaps project to different extrinsic targets (see Shipp & Zeki, 1989).

Although we did not note any difference between layer 5 neurons with different length apical dendrites, we did identify a novel type of layer 5 "backbranching" pyramidal neuron with distinctive dendritic and axonal arbors. Only three of 16 layer 5 neurons in our sample belong to this type and these are the only layer 5 cells that project to the white matter. This observation raises the possibility that, like layer 6 neurons in macaque V1, only a minority are projection neurons (Fitzpatrick et al., 1994; Wiser & Callaway, 1996). Likely targets of the layer 5 projection neurons are the superior colliculus or the pulvinar nucleus (Lund et al., 1975), but the possibility that these cells project to other target(s) cannot be ruled out. Since, we have not sampled any "tall" layer 5 pyramids (Lund & Boothe, 1975; Valverde, 1985), it is not known whether they are projection neurons or how they might contribute to local circuits in V1.

Acknowledgments

We thank Janet Lieber for expert technical assistance; Dr. Carl Lupica for sharing his equipment, time, and expertise; Dr. Joseph Callaway, Dr. Carl Lupica, and Atomu Sawatari for assistance labeling neurons; and Lori Greiner for assistance with animals. This work was supported

by NIH Grant EY10742, the Esther A. and Joseph Klingenstein Fund, and NIH Training Grant T32 HD07408 (A.K.W.).

References

ANDERSON, J.C., MARTIN, K.A.C. & WHITTERIDGE, D. (1993). Form, function, and intracortical projections of neurons in the striate cortex of the monkey *Macacus nemestrinus*. *Cerebral Cortex* **3**, 412-420.

BLANTON, M.G., LO TURCO, J.J. & KRIEGSTEIN, A.R. (1989). Whole cell recording from neurons in slices of reptilian and mammalian cerebral cortex. *Journal of Neuroscience Methods* **30**, 203-210.

BLASDEL, G.G. & FITZPATRICK, D. (1984). Physiological organization of layer 4 in macaque striate cortex. *Journal of Neuroscience* **4**, 880-895.

BLASDEL, G.G., LUND, J.S. & FITZPATRICK, D. (1985). Intrinsic connections of macaque striate cortex: Axonal projections of cells outside lamina 4C. *Journal of Neuroscience* **5**, 3350-3369.

CALLAWAY, E.M. & KATZ, L.C. (1992). Development of axonal arbors of layer 4 spiny neurons in cat striate cortex. *Journal of Neuroscience* **12**, 570-582.

CALLAWAY, E.M. (1993). Organization of functional stream specific local circuits in the primary visual cortex of newborn macaque monkeys. *Society for Neuroscience Abstracts* **19**, 240.

CASAGRANDE, V.A. & KAAS, J.H. (1995). The afferent, intrinsic, and efferent connections of primary visual cortex in primates. In *Cerebral Cortex, Vol. 10*, ed. PETERS, A. & ROCKLAND, K.S., pp. 201-259. New York: Plenum Press.

FITZPATRICK, D., LUND, J.S. & BLASDEL, G.G. (1985). Intrinsic connections of macaque striate cortex: Afferent and efferent connections of lamina 4C. *Journal of Neuroscience* **5**, 3329-3349.

FITZPATRICK, D., USREY, W.M., SCHOFIELD, B.R. & EINSTEIN, G. (1994). The sublaminar organization of corticogeniculate neurons in layer 6 of macaque striate cortex. *Visual Neuroscience* **11**, 307-315.

GILBERT, C.D. (1983). Microcircuitry of the visual cortex. *Annual Review of Neuroscience* **6**, 217-247.

GILBERT, C.D. & WIESEL, T.N. (1979). Morphology and intracortical projections of functionally characterized neurones in the cat visual cortex. *Nature* **280**, 120-125.

GILBERT, C.D. & WIESEL, T.N. (1983). Clustered intrinsic connections in cat visual cortex. *Journal of Neuroscience* **3**, 1116-1133.

HORTON, J.C. (1984). Cytochrome oxidase patches: A new cytoarchitectonic feature of monkey visual cortex. *Philosophic Transcript of the Royal Society B* (London) **304**, 199-253.

HORTON, J.C. & HOCKING, D.R. (1996). An adult-like pattern of ocular dominance columns in striate cortex of newborn monkeys prior to visual experience. *Journal of Neuroscience* **16**, 1791-1807.

HUBENER, M. & BOLZ, J. (1992). Relationships between dendritic morphology and cytochrome oxidase compartments in monkey striate cortex. *Journal of Comparative Neurology* **324**, 67-80.

KATZ, L.C. (1987). Local circuitry of identified projection neurons in cat visual cortex brain slices. *Journal of Neuroscience* **7**, 1223-1249.

KATZ, L.C., GILBERT, C.D. & WIESEL, T.N. (1989). Local circuits and ocular dominance columns in monkey striate cortex. *Journal of Neuroscience* **9**, 1389-1399.

LACHICA, E.A., BECK, P.D. & CASAGRANDE, V.A. (1992). Parallel pathways in macaque monkey striate cortex: Anatomically defined columns in layer III. *Proceeding of the National Academy of Sciences of the U.S.A.* **89**, 3566-3570.

LIVINGSTONE, M.S. & HUBEL, D.H. (1984). Specificity of intrinsic connections in primate primary visual cortex. *Journal of Neuroscience* **4**, 2830-2835.

LUND, J.S. (1973). Organization of neurons in the visual cortex, area 17, of the monkey (*Macaca mulatta*). *Journal of Comparative Neurology* **147**, 455-496.

LUND, J.S. (1987). Local circuit neurons of macaque monkey striate cortex. I. Neurons of laminae 4C and 5A. *Journal of Comparative Neurology* **257**, 60-92.

LUND, J.S. (1988). Anatomical organization of macaque monkey striate visual cortex. *Annual Review of Neuroscience* **11**, 253-288.

LUND, J.S. & BOOTHE R.G. (1975). Interlaminar connections and pyramidal neuron organisation in the visual cortex, area 17, of the macaque monkey. *Journal of Comparative Neurology* **159**, 305-334.

LUND, J.S., LUND, R.D., HENDRICKSON, A.E., BUNT, A.H. & FUCHS, A.F. (1975). The origin of efferent pathways from the primary visual cortex, area 17, of the macaque monkey as shown by retrograde transport of horseradish peroxidase. *Journal of Comparative Neurology* **164**, 287-303.

LUND, J.S., BOOTHE, R.G. & LUND, R.D. (1977). Development of neurons in the visual cortex of the monkey (*Macaca nemestrina*): A Golgi study from fetal day 127 to postnatal maturity. *Journal of Comparative Neurology* **176**, 149-188.

LUND, J.S., YOSHIOKA, T. & LEVITT, J.B. (1993). Comparison of intrinsic connectivity in different areas of macaque monkey cerebral cortex. *Cerebral Cortex* **3**, 148-162.

MARTIN, K.A.C. (1984). Neuronal circuits in cat striate cortex. In *Cerebral Cortex, Vol. 2*, ed. JONES, E.G. & PETERS, A., pp. 241-284. New York: Plenum Press.

MARTIN, K.A.C. & WHITTERIDGE, D. (1984). Form, function and intracortical projections of spiny neurons in the striate cortex of the cat. *Journal of Physiology* **353**, 463-504.

MATES, S.L. & LUND, J.S. (1983). Neuronal composition and development in lamina 4C of monkey striate cortex. *Journal of Comparative Neurology* **221**, 60-90.

MCGUIRE, B.A., GILBERT, C.D., RIVLIN, P.K. & WIESEL, T.N. (1991). Targets of horizontal connections in macaque primary visual cortex. *Journal of Comparative Neurology* **305**, 370-392.

MERIGAN, W.H. & MAUNSELL, J.H.R. (1993). How parallel are the visual pathways? *Annual Review of Neuroscience* **16**, 369-402.

NEALEY, T.A. & MAUNSELL, J.H.R. (1994). Magnocellular and parvocellular contributions to the responses of neurons in macaque striate cortex. *Journal of Neuroscience* **14**, 2069-2079.

SAINT MARIE, R.L. & PETERS, A. (1985). The morphology and synaptic connections of spiny stellate neurons in monkey visual cortex (area 17): A Golgi-electron microscopic study. *Journal of Comparative Neurology* **233**, 213-235.

SAWATARI, A. & CALLAWAY, E.M. (1996). Convergence of magno- and parvocellular pathways in layer 4B of macaque primary visual cortex. *Nature* **380**, 442-446.

SHIPP, S. & ZEKI, S. (1989). The organization of connections between areas V5 and V1 in macaque monkey visual cortex. *European Journal of Neuroscience* **1**, 309-332.

USREY, W.M. & FITZPATRICK, D. (1994). Laminar specificity in the relay of magnocellular and parvocellular streams to the superficial and deep layers of macaque striate cortex. *Society for Neuroscience Abstracts* **20**, 1578.

VALVERDE, F. (1985). The organizing principles of the primary visual cortex in the monkey. In *Cerebral Cortex, Vol. 3*, ed. JONES, E.G. & PETERS, A., pp. 207-257. New York: Plenum Press.

WISER, A.K. & CALLAWAY, E.M. (1996). Contributions of individual layer 6 pyramidal neurons to local circuitry in macaque primary visual cortex. *Journal of Neuroscience* **16**, 2724-2739.

YOSHIOKA, T., LEVITT, J.B. & LUND, J.S. (1994). Independence and merger of thalamocortical channels within macaque monkey primary visual cortex: Anatomy of interlaminar projections. *Visual Neuroscience* **11**, 467-489.